Inorg. Chem. **2002**, *41*, 5706–5715

Structure, Insertion Electrochemistry, and Magnetic Properties of a New Type of Substitutional Solid Solutions of Copper, Nickel, and Iron Hexacyanoferrates/Hexacyanocobaltates

Antje Widmann, Heike Kahlert,* Irena Petrovic-Prelevic, Harm Wulff, J. V. Yakhmi,† Nitin Bagkar,† and Fritz Scholz

Ernst-Moritz-Arndt-Universität Greifswald, Institut für Chemie und Biochemie, Soldmannstrasse 23, D-17489 Greifswald, Germany

Received March 1, 2002

Substitutional solid solutions of metal hexacyanometalates in which low-spin iron(III) and cobalt(III) ions populate the carbon-coordinated sites were synthesized and studied by powder diffraction including Rietveld refinement, cyclic voltammetry of immobilized microparticles, diffuse reflection vis-spectrometry, and magnetization techniques. The continuous solid solution series of potassium copper(II), potassium nickel(II), and iron(III) [(hexacyanoferrate(III))$_{1-x}$ (hexacyanocobaltate(III))$_x$] show that the substitution of low-spin iron(III) by cobalt(III) in the hexacyanometalate units more strongly affects the formal potentials of the nitrogen-coordinated copper(II) and high-spin iron(III) ions than those of the remaining low-spin iron(III) ions. In the case of copper(II) and iron(III) [(hexacyanoferrate(III))$_{1-x}$(hexacyanocobaltate(III))$_x$] the peak currents decrease much more than can be explained by stoichiometry, indicating that the charge propagation is slowed by the substitution of low-spin iron(III) by cobalt(III). The Rietveld refinement of all compounds confirmed the structure initially proposed by Keggin for Prussian blue and contradicts the structure described later by Ludi. The dependencies of lattice parameters on composition exhibit in all series of solid solutions studied similar, although small, deviations from ideality, which correlate with the electrochemical behavior. Finally, a series of solid solutions of the composition $KNi_{0.5}^{II}Cu_{0.5}^{II}[Fe^{III}(CN)_6]_{1-x}[Co^{III}(CN)_6]_x$, where both the nitrogen- and carbon-coordinated metal ions are mixed populated and were synthesized and characterized. These are the first examples of solid solutions of metal hexacyanometalates with four different metal ions, where both the nitrogen- and the carbon-coordinated sites possess a mixed population.

Introduction

Transition metal hexacyanometalates form a class of zeolitic inorganic compounds that have been studied extensively because of their outstanding properties. Many of these compounds exhibit a reversible insertion electrochemistry[1−4] and possess electrocatalytic activity,[5−8] electrochromism,[9−15] and the capability to be used in rechargeable batteries.[16−20] Some transition metal hexacyanometalates are high-temperature ferromagnets.[21−28] Most metal hexacyanometalates have a cubic structure as depicted in Figure 1. Metal ions are

* To whom correspondence should be addressed. Tel.: +49(0)3834-86-4454. Fax: +49(0)3834-864451. E-mail: hkahlert@mail.uni-greifswald.de.

† Technical Physics & Prototype Engineering Division, Bhabha Atomic Research Centre, Mumbai (Bombay) 400085, India.

(1) Siperkow, M. L.; Kuwana, T. *Electrochim. Acta* **1987**, *32*, 765−771.
(2) Engel, D.; Grabner, E. W. *Ber. Bunsen-Ges. Phys. Chem.* **1985**, *89*, 982−986.
(3) Itaya, I.; Uchida, I. *Acc. Chem. Res.* **1986**, *19*, 162−168.
(4) Scholz, F.; Dostal, A. *Angew. Chem., Int. Ed. Engl.* **1995**, *34*, 2685−2687.
(5) Sinha, S.; Humphrey, B. D.; Bocarsly, A. B. *Inorg. Chem.* **1984**, *23*, 203−212.
(6) Dong, S.; Che, G. *J. Electroanal. Chem.* **1991**, *315*, 191.
(7) Weissenbacher, M.; Kalcher, K.; Greschoing, H.; Ng, W.; Chan, W. H.; Volgaropoulos, A. *Fresenius J. Anal. Chem.* **1992**, *344*, 87−92.
(8) Shankaran, D. R.; Narayanan, S. S. *Bull. Electrochem.* **1998**, *14*, 267−270.
(9) Viehbeck, A.; DeBerry, D. W. *J. Electrochem. Soc.* **1985**, *132*, 1369−1375.
(10) Kellawi, H.; Rosseinsky, D. R. *J. Electroanal. Chem.* **1982**, *131*, 373−376.
(11) Itaya, K.; Shibayama, K.; Akahoshi, H.; Toshima, S. *J. Appl. Phys.* **1982**, *53*, 804−805.
(12) DeBerry, D. W.; Viehbeck, A. *J. Electrochem. Soc.* **1983**, *130*, 249−251.
(13) Mortimer, R. J. *J. Electrochem. Soc.* **1991**, *138*, 633.
(14) Greenberg, C. B. *Thin Solid Films* **1994**, *251*, 81−93.
(15) Monk, P. M. S.; Mortimer, R. J.; Rosseinsky, D. R. *Electrochromism: Fundamentals and Applications*; VCH: Weinheim, 1995.
(16) Neff, V. D. *J. Electrochem. Soc.* **1985**, *132*, 1382−1384.
(17) Grabner, E. W.; Kalwellis-Mohn, S. *J. Appl. Electrochem.* **1987**, *17*, 653−656.
(18) Kalwellis-Mohn, S.; Grabner, E. W. *Electrochim. Acta* **1989**, *34*, 1265−1269.
(19) Kuwabara, K.; Nunome, J.; Sugiyama, K. *Solid State Ionics* **1991**, *48*, 303.
(20) Jayalakshmi, M.; Scholz, F. *J. Power Sources* **2000**, *91*, 217−223.

10.1021/ic0201654 CCC: $22.00
Published on Web 10/04/2002

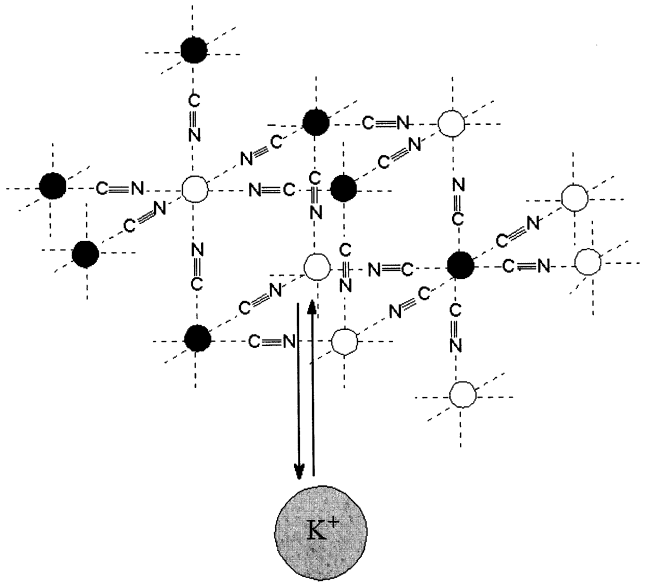

Figure 1. Schematic description of the structure of metal hexacyanometalates (●: Fe^{3+}, Co^{3+}; ○: Cu^{2+}, Ni^{2+}, Fe^{3+}).

situated at the corners of the cube and they are octahedrally coordinated by the nitrogen or carbon end of the cyanide groups; that is, the cyanide groups are bridging the metal ions along the cube edges. Depending on the number of charges of the nitrogen- and carbon-coordinated metal ions, a certain amount of cations can be placed at interstitial positions for charge compensation. These interstitial metal ions may be the same as the nitrogen- and carbon-coordinated metal ions, or they may be alkali metal ions. The analysis of the structure of metal hexacyanometalates (especially of Prussian Blue as the most famous compound) with a range of different techniques has been described in the literature over the past decades.[29−38] Ludi and co-workers described the structure of single crystals of Prussian blue as a highly disordered cubic cell, but in fact they obtained these crystals as a potassium-free compound by slow crystallization from a highly concentrated hydrochloric acid.[30,31] However, this structure model holds true only for alkali-free samples. The results of their study cannot be applied to alkali ion-containing compounds.

In electrochemical reactions of metal hexacyanometalates an electron transfer is accompanied by the transfer of cations between the solid compound and the adjacent solution. Because these electrochemical reactions are in all known cases reversible, the compounds are model systems for insertion electrochemical reactions.

Very recently, a theoretical explanation has been given for the dependence of the formal potentials of the hexacyanometalate system on the properties of the metal ions that build up the solid compounds.[39] This offers the possibility to tune the electrochemical properties of metal hexacyanometalates. Solid solutions are attractive for the deliberate change in the properties because the tuning can be achieved in a continuous way. The knowledge of solid solutions of hexacyanometalates is so far confined to compounds where the nitrogen-coordinated metal ions were substituted. Thus, $K_2Cu_{1-x}Ni_x[Fe(CN)_6]$, $K_2Ni_{1-x}Pd_x[Fe(CN)_6]$, $K_2Ni_{1-x}Co_x[Fe(CN)_6]$, and $K_{2-x}Fe_{1-x}Ni_x[Fe(CN)_6]$,[40] and the complicated system cadmium/iron hexacyanoferrate[41] have been studied in detail.[42−44] However, there are no data available on compounds where the carbon-coordinated metal ion, that is, the central metal ion in the hexacyanometalate unit, was substituted. This fact prompted us to study the electrochemical properties of the following transition metal hexacyanoferrates/hexacyanocobaltates:

$$K\mathrm{Cu^{II}}[\mathrm{Fe^{III}}(CN)_6]_{1-x}[\mathrm{Co^{III}}(CN)_6]_x \quad (1)$$

$$K\mathrm{Ni^{II}}[\mathrm{Fe^{III}}(CN)_6]_{1-x}[\mathrm{Co^{III}}(CN)_6]_x \quad (2)$$

$$\mathrm{Fe^{III}}[\mathrm{Fe^{III}}(CN)_6]_{1-x}[\mathrm{Co^{III}}(CN)_6]_x \quad (3)$$

The compounds in these series represent a new type of substitutional solid solutions that have not been described before. For the sake of comparison, also a series of mixed crystals was synthesized where both the nitrogen- and the carbon-coordinated metal ions are mixed:

$$K\mathrm{Ni}_{0.5}\mathrm{II}\mathrm{Cu}_{0.5}\mathrm{II}[\mathrm{Fe^{III}}(CN)_6]_{1-x}[\mathrm{Co^{III}}(CN)_6]_x$$

The compounds of this series are the first examples of well-defined solid solutions of hexacyanometalates with four

(21) Sato, O.; Iyoda, T.; Fujishima, A.; Hashimoto, K. *Science* **1996**, *271*, 49−55.
(22) Entley, W. R.; Girolami, G. S. *Science* **1995**, *268*, 397−401.
(23) Ohkoshi, S.; Abe, Y.; Fujishima, A.; Hashimoto, K. *Phys. Rev. Lett.* **1999**, *82*, 1285−1288.
(24) Verdaguer, M. *Polyhedron* **2001**, *20*, 1115−1128.
(25) Ohkoshi, S.; Mizuno, M.; Hung, G.; Hashimoto, K. *J. Phys. Chem. B* **2000**, *104*, 9365−9367.
(26) Mallah, T.; Thiébaut, S.; Verdaguer, M.; Veillet, P. *Science* **1993**, *262*, 1554−1557.
(27) Ng., C. W.; Ding, J.; Shi, Y.; Gan, L. M. *J. Phys. Chem. Solids* **2001**, *62*, 767−775.
(28) Salah El Fallah, M.; Ribas, J.; Solans, X.; Font-Bardia, M. *J. Chem. Soc., Dalton Trans*. **2001**, 247−250.
(29) Herren, F.; Fischer, P.; Ludi, A.; Haelg, W. *Inorg. Chem*. **1980**, *19*, 956−959.
(30) Ludi, A.; Güdel, H. U. *Struct. Bonding* **1973**, *14*, 1−21.
(31) Buser, H. J.; Schwarzenbach, D.; Petter, W.; Ludi, A. *Inorg. Chem*. **1977**, *16*, 2704−2710.
(32) Ayers, J. B.; Waggoner, W. H. *J. Inorg. Nucl. Chem*. **1971**, *33*, 721−733.
(33) Siebert, H.; Nuber, B.; Jentsch, W. *Z. Anorg. Allg. Chem*. **1981**, *474*, 96−104.
(34) Zubkov, V. G.; Tyutyunnik, A. P.; Berger, I. F.; Maksimova, L. G.; Denisova, T. A.; Polyakow, E. V.; Kaplan, I. G.; Voronin, V. I. *Solid State Sci.* **2001**, *3*, 361−367.
(35) Bonnette, A. K.; Gandy, S. E. *J. Chem. Educ.* **1981**, *58*, 355−357.
(36) Ikeshoji, T.; Iwasaki, T. *Inorg. Chem*. **1988**, *27*, 1124−1126.
(37) Ryzhkov, M. V.; Denisova, T. A.; Zubkov, V. G.; Maksimova, L. G. *J. Struct. Chem*. **2000**, *41*, 927−933.
(38) (a) Scholz, F., Meyer, B. Voltammetry of Solid Microparticles Immobilised on Electrode Surfaces. In *Electroanalytical Chemistry*; Bard, A., Rubinstein, I., Eds.; Marcel Dekker: New York, 1998; Vol 20. (b) Fiedler, D. A.; Scholz, F.; Electrochemical Studies of Solid Compounds and Materials. In *Electroanalytical Methods*; Scholz, F., Ed.; Springer: Berlin, 2002.
(39) Bàrcena Soto, M.; Scholz, F. *J. Electroanal. Chem*., in press.
(40) Reddy, S. J.; Dostal, A.; Scholz, F. *J. Electroanal. Chem*. **1996**, *403*, 209−212.
(41) Zakharschuk, N. F.; Nammov, N.; Stösser, R.; Schröder, U.; Scholz, F.; Mehner, H. *J. Solid State Electrochem*. **1999**, *3*, 264−276.
(42) Schwudtke, D.; Stösser, R.; Scholz, F. *Electrochem. Comm*. **2000**, *2*, 301−306.

different metal ions populating both the nitrogen- and the carbon-coordinated sites.

In this paper, the symbol [*hcf*] stands always for $[Fe^{III}(CN)_6]^{3-}$ ions and the symbol [*hcc*] stands for $[Co^{III}(CN)_6]^{3-}$ ions. The synthesized materials were generally the hexacyanoferrates(III) and hexacyanocobaltates(III) because these can be obtained by precipitation with a much better crystallinity than the corresponding hexacyanoferrate(II) salts. The hexacyanocobaltate(II) salts are not accessible by synthesis.

Experimental Section

(a) Equipment. Electrochemical measurements were performed using an AUTOLAB system with a PGSTAT 20 (Eco-Chemie, Utrecht, The Netherlands) in conjunction with a three-electrode system and a personal computer (IBM-compatible). The reference electrode was an Ag/AgCl electrode (3 M KCl) (Metrohm, Herisau, Switzerland) with a potential of 0.208 V vs SHE at 25 °C. A platinum wire served as an auxiliary electrode. Working electrodes used in this study were paraffin-impregnated graphite electrodes (PIGE), prepared from graphite rods (electrodes for spectrographic analysis, VEB Elektrokohle Lichtenberg, Berlin, Germany) impregnated in molten paraffin.[38]

The diffuse reflectance spectra were measured using a Leitz Laborlux 12 Pol S incident light microscope (Leica Microsystems, Wetzlar, Germany) with two crossed linear polarized filters to minimize the specular reflectance. The microscope was coupled via fiber optics with a transputer-integrated diode array system (TIDAS) (J & N Analytische Mess-und Regeltechnik, Ahlen, Germany) with a spectral range of 400−800 nm and a personal computer (IBM-compatible).

X-ray diffraction data were collected on a D5000 Siemens diffractometer (Siemens, Germany) using Bragg−Brentano geometry. Cu K_α radiation was used. To suppress the Cu K_β and fluorescence radiation, the diffractometer is equipped with a secondary graphite monochromator. The diffraction patterns for the Rietveld refinement were scanned over the angular range of 10−120°/2θ with a step length of 0.03°/2θ. The counting times were 20 s/step. The structure solution and refinement were performed on the base of the model from Keggin and Miles[45] using the programs FULLPROF and GFOUR.[46,47]

The Prussian blue analogue samples were subjected to magnetization measurements as a function of temperature, *M* vs *T*, as well as applied field, *M* vs *H*, using a Vibration Sample Magnetometer Model 4500 (E.G. & G. Princeton Applied Research). The temperature dependence of magnetization was studied by carrying out field-cooled magnetization (FCM), zero field-cooled magnetization (ZFCM), and remanent magnetization (REM) on the sample. FCM data were obtained after cooling the sample in 500 Oe applied field and then recording the magnetization while warming the sample up from 4.5−35 K, keeping the field on. The ZFCM data were obtained by cooling the sample down to 4.5 K in the zero applied field, then switching the applied field on (500 Oe) at this temperature, and recording the magnetization while warming the sample up. REM data were collected after cooling the sample to 4.5 K under the applied field of 500 Oe and recording the data while warming the sample up after reducing the field to zero. The field dependence of the magnetization *M* vs *H* plots were recorded at 4.5 K under an applied field of −9000 to 9000 Oe. The hysteresis loops obtained were typical of long-range magnetically ordered (ferromagnetic) samples with varying coercive field values for different samples.

(b) Electrode Preparation. The solid compounds were studied by employing cyclic voltammetry as microparticles attached to the surface of a paraffin-impregnated graphite electrode (cf. the *voltammetry of immobilized particles*)[38] in 0.1 M KNO_3 solution with a scan rate of 50 mV/s. The sample preparation was carried out as follows: 1−3 mg of the sample powder was placed on a glass plate. The electrode was gently rubbed over the material to immobilize it at the electrode surface. After measurement the electrode surface was cleaned by rubbing it over abrasive paper and finally polishing it on white printing paper.

(c) Chemicals. The used chemicals were all of p.a. quality and purchased from Merck (Germany): $K_3[Fe(CN)_6]$, $CuCl_2$, KNO_3, $CoCl_2 \cdot 6H_2O$, KCN, $Fe(NO_3)_3 \cdot 9H_2O$, and $Ni(NO_3)_2 \cdot 6H_2O$. Bidistilled water was used throughout. $K_3[Co(CN)_6]$ was synthesized following a literature procedure.[48]

(d) Synthesis of $KNi^{II}[hcf]_{1-x}[hcc]_x$, $Fe^{III}[hcf]_{1-x}[hcc]_x$, and $KCu^{II}[hcf]_{1-x}[hcc]_x$. It is crucial to perform the synthesis exactly as described, especially in the order in which reagent solutions are added, because otherwise different products may precipitate. The substitutional solid solutions were synthesized as a continuous series by changing the content of cobalt(III) in 10% steps. To synthesize $KNi^{II}[hcf]_{1-x}[hcc]_x$ and $KCu^{II}[hcf]_{1-x}[hcc]_x$, the mixed solutions of $K_3[Co(CN)_6]$ and $K_3[Fe(CN)_6]$ were added dropwise to the stirred 0.2 mol L^{-1} solution of $CuCl_2$ with an excess of KNO_3 or to a 0.2 mol L^{-1} solution of $Ni(NO)_2 \cdot 6H_2O$ with an excess of KNO_3. To obtain $Fe^{III}[hcf]_{1-x}[hcc]_x$, the mixed solutions of $K_3[Co(CN)_6]$ and $K_3[Fe(CN)_6]$ were added dropwise to the stirred 0.2 mol L^{-1} solution of $Fe(NO_3)_3 \cdot 9H_2O$ in 0.1 M HCl. After addition, the solution was heated for 15 min. All precipitates were allowed to stand for 1 night and were then centrifuged. After the precipitates were washed twice with bidistilled water, they were dried at 40 °C. The dried products formed glassy solids that were milled in a mortar and washed carefully several times with bidistilled water to remove any remaining traces of potassium nitrate and chloride.

(e) Synthesis of $KNi_{0.5}^{II}Cu_{0.5}^{II}[hcf]_{1-x}[hcc]_x$. This series of mixed crystals was synthesized as described in (d) by using a mixed solution of 0.1 mol L^{-1} $Ni(NO)_2 \cdot 6H_2O$ and 0.1 mol L^{-1} $CuCl_2$. The following steps were conducted as described above.

(f) Chemical Analysis. C, H, and N elemental analysis and AAS analysis of metals confirmed in all cases the composition of compounds as indicated.

Results and Discussion

X-ray Diffraction Analysis. All compounds investigated here are polycrystalline. The powder diffractograms of the compounds $KCu^{II}[hcf]$, $KNi^{II}[hcf]$, and $Fe^{III}[hcf]$ are shown in Figure 2. These experimental data match very well the simulated patterns of the proposed structure model of Keggin and Miles.[44] Therefore, it was possible to obtain information on the space group and the position of the potassium ions in the unit cell. Assuming the spacegroup $Fm\bar{3}m$, all reflections

(43) Kulesza, P. J.; Malik, A. M.; Schmidt, R.; Smolinska, A.; Miecznikowski, K.; Zamponi, S.; Czerwinski, A.; Berrettoni, M.; Marassi, R. *J. Electroanal. Chem*. **2000**, *487*, 57−65.
(44) Kulesza, P. J.; Malik, A. M.; Skorek, J.; Miecznikowski, K.; Zamponi, S.; Berrettoni, M.; Giorgetti, M.; Marassi, R. *J. Electrochem. Soc*. **1999**, *146*, 3757−3761.
(45) Keggin, J. F.; Miles, F. D. *Nature (London)* **1936**, *137*, 577−578.
(46) Rodriguez-Carvajal, J. In *Collected Abstracts of Powder Diffraction Meeting*, Toulouse, France, 1990; p 127.
(47) Rodriguez-Carvajal, J.; Roisnel, T. *Newsletter* **1998**, *20*, 35−36.
(48) Brauer, G. *Handbuch der präparativen anorganischen Chemie*; Ferdinand Enke Verlag: Stuttgart, 1954.

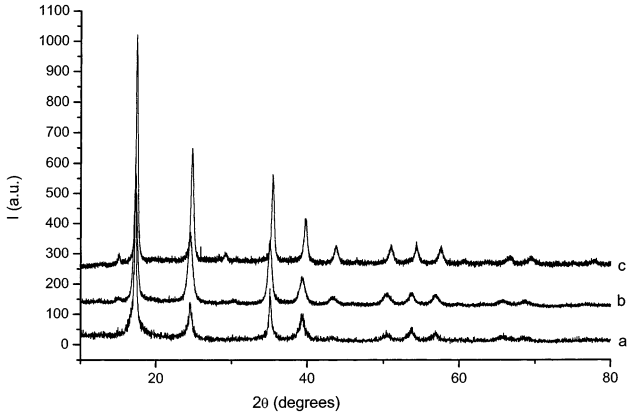

Figure 2. Experimental powder data of (a) $KCu^{II}[hcf]$, (b) $KNi^{II}[hcf]$, and (c) $Fe^{III}[hcf]$.

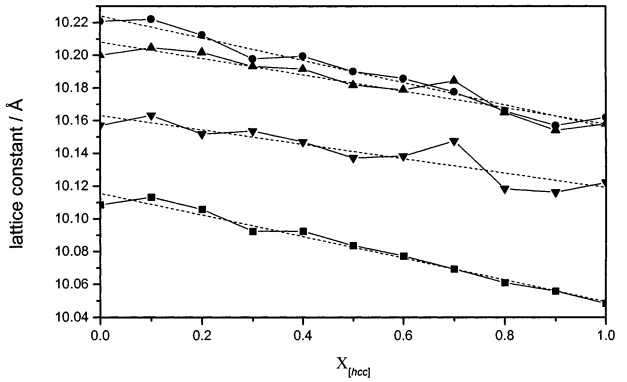

Figure 3. Lattice constants of (●) $KNi^{II}[hcf]_{1-x}[hcc]_x$, (▲) $Fe^{III}[hcf]_{1-x}[hcc]_x$, (■) $KCu^{II}[hcf]_{1-x}[hcc]_x$, and (▼) $KNi_{0.5}{}^{II}Cu_{0.5}{}^{II}[hcf]_{1-x}[hcc]_x$ dependent on the molar ratio of cobalt. The dashed lines result from a linear fitting.

can be indexed and no additional reflections were observed. There is no preferential orientation in the polycrystalline samples; however, differences in the absolute and relative integral intensities as well as in the profile forms can be observed.

The series of compounds $KCu^{II}[hcf]_{1-x}[hcc]_x$, $KNi^{II}[hcf]_{1-x}[hcc]_x$, and $Fe^{III}[hcf]_{1-x}[hcc]_x$ with $0 \le x \le 1$ show in principle the same diffraction patterns as shown in Figure 2 with systematic shifts in the peak positions. In Figure 3 the lattice constants of these compounds are plotted versus hexacyanocobaltate(III) content. Generally, the lattice constants follow Vegards rule (lattice constants vary linearly with the composition of the solid solutions); however, the dependence shows a very interesting fine structure (deviation from linearity) that is observed for all systems. This deviation will be discussed later in conjunction with the electrochemistry. However, the general agreement with Vegards rule and the similarity of the diffraction patterns indicate that solid solutions have been formed. In all the mixed crystal systems the lattice constants decrease with rising molar ratio of hexacyanocobaltate(III). This behavior is in agreement with the difference in the ionic radii of octahedrally coordinated low-spin Fe^{3+} (69 pm) and Co^{3+} (68.5 pm) ions.[49] Not yet understood are the appreciable higher lattice constants of the solid solutions of $KNi^{II}[hcf]_{1-x}[hcc]_x$ and $Fe^{III}[hcf]_{1-x}[hcc]_x$ compared to the solid solutions of $KCu^{II}[hcf]_{1-x}[hcc]_x$. The ionic radii of octahedrally coordinated Cu^{2+} is 87 pm, that for Ni^{2+} is 83 pm, and that for high-spin Fe^{3+} is 78.5 pm.[49]

Table 1. Crystal Structure Data for $KCu^{II}[hcf]_{0.3}[hcc]_{0.7}$ (Space Group $Fm\bar{3}m$, $a_0 = 10.0754(2)$ Å)

atom	site	*x*	*y*	*z*	B_{iso}	SOF
Fe	4a	0	0	0	3.59(59)	0.3
Co	4a	0	0	0	3.59(59)	0.7
Cu	4b	0.5	0.5	0.5	1.36(37)	1
K	8c	0.25	0.25	0.25	17.04(89)	0.5
C	24e	0.2052(16)	0	0	4.79(1.0)	1
N	24e	0.3140(17)	0	0	3.14(1.0)	1

Table 2. Crystal Structure Data for $KNi^{II}[hcf]_{0.3}[hcc]_{0.7}$ (Space Group $Fm\bar{3}m$, $a_0 = 10.1818(8)$ Å)

atom	site	*x*	*y*	*z*	B_{iso}	SOF
Fe	4a	0	0	0	7.12(84)	0.3
Co	4a	0	0	0	7.12(84)	0.7
Ni	4b	0.5	0.5	0.5	5.99(70)	1
K	96k	0.247(25)	0.2997(37)	0.2997(37)	9.01(1.0)	0.04166
C	24e	0.2145(11)	0	0	4.20 (77)	1
N	24e	0.3231(12)	0	0	6.53(67)	1

Attempts to refine the structure of $Fe^{III}[hcf]_{1-x}[hcc]_x$ were not completely successful, probably due to significant differences in the profile forms and strong decrease of the intensities in the high-angle range. R_{wp} factors and χ^2 were high ($R_{wp} > 18\%$ and $\chi^2 > 2$) especially for mixed crystals with a high molar ratio of hexacyanocobaltate(III). The results of the Rietveld refinement will be exemplified for the mixed crystals $KCu^{II}[hcf]_{0.3}[hcc]_{0.7}$ and $KNi^{II}[hcf]_{0.3}[hcc]_{0.7}$. The parameters finally obtained are $R_{wp} = 10.4$, $R_{exp} = 9.42$, $\chi^2 = 1.21$, and DW = 1.802 for $KCu^{II}[hcf]_{0.3}[hcc]_{0.7}$ and $R_{wp} = 16.3$, $R_{exp} = 12.4$, $\chi^2 = 1.72$, and DW = 1.217 for $KNi^{II}[hcf]_{0.3}[hcc]_{0.7}$. The crystal structure data are summarized in Tables 1 and 2. The most significant result from the structure refinement is the obvious disorder of the potassium sites (Figure 4 a and b). In the compound $KCu^{II}[hcf]_{0.3}[hcc]_{0.7}$ the potassium ions occupy statistically one-half of the 8-fold sites but with a high value of the isotropic temperature factor. The K−Cu bond length is 436 pm. The high-temperature factor suggests a smudgy position of the potassium ions in the channels of the hexacyanometalates (Figure 4a). In the compound $KNi^{II}[hcf]_{0.3}[hcc]_{0.7}$ the potassium ions occupy partially the 96 k site (4/96). This is equivalent also to stoichiometric $KNi^{II}[hcf]_{0.3}[hcc]_{0.7}$. The shortest K−Ni bond length is 387 pm, that is, significantly smaller than that in the K−Cu compound (Figure 4b). This eccentrical position of the countercation was described by Bocarsly and co-workers[50] for sodium-containing nickel hexacyanoferrate(II).

Ludi and co-workers[30,31] discussed the presence of water as a part of the structure in $Fe_4[Fe(CN)_6]_3 \cdot xH_2O$ and of "free" water in the single crystals. Thermo analysis of our samples of $KCu^{II}[hcf]_{1-x}[hcc]_x$ and $KNi^{II}[hcf]_{1-x}[hcc]_x$ show a loss of mass that is smaller in the case of $KCu^{II}[hcf]_{1-x}[hcc]_x$ than in the case of $KNi^{II}[hcf]_{1-x}[hcc]_x$. For example, the X-ray density of the compound $KCu^{II}[hcf]_{0.6}[hcc]_{0.4}$ following from Rietveld refinement is $\rho_{x-ray} = 2.039$ g/cm^3. The experimental density obtained by pycnometric measurements is ρ_{exp}

(49) Shannon, R. D. *Acta Crystallogr.* **1976**, *A32*, 751.
(50) Kelly, M. T.; Arbuckle-Keil, G. A.; Johnson, L. A.; Su, E. Y.; Amos, L. J.; Chun, J. K. M.; Bocarlsy, A. B. *J. Electroanal. Chem.* **2001**, *500*, 311−321.

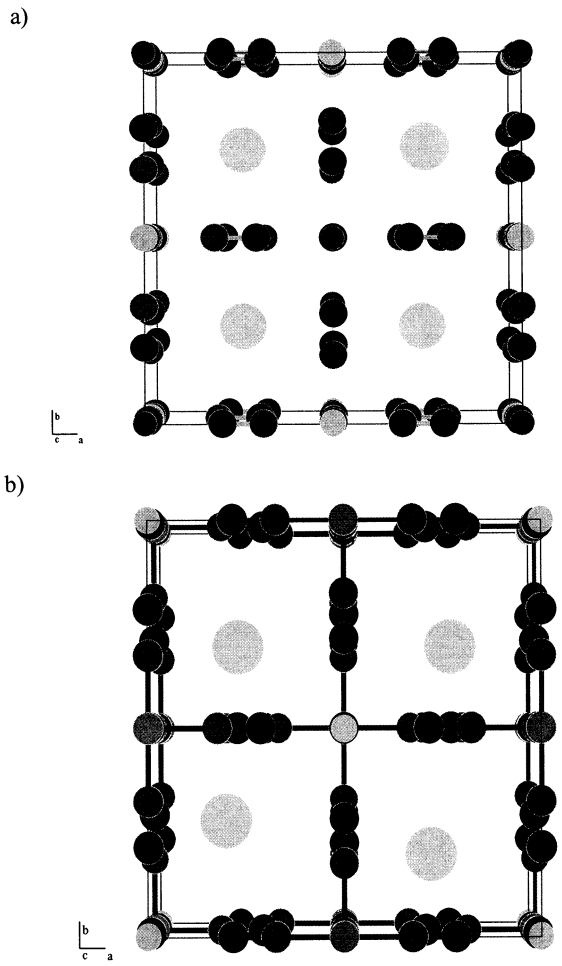

Figure 4. (a) Crystal structure of $KCu^{II}[hcf]_{0.3}[hcc]_{0.7}$. (b) Crystal structure of $KNi^{II}[hcf]_{0.3}[hcc]_{0.7}$.

$= 1.74$ g/cm^3. Upon heating at 300 °C, the compound loses 25% of mass. When the mass loss by heating the samples up to 300 °C is ascribed to adsorbed and adhering water, this almost exactly accounts for the difference between these two densities (in the pycnometric measurement the adhering water decreases the apparent density). Hence, the formula $KCu^{II}[hcf]_{0.6}[hcc]_{0.4}\cdot 4.5H_2O$ just indicates the amount of water adhering to the crystals. This interpretation was also proved by X-ray diffraction of the compounds before and after DTA/TG measurements, showing identical diffraction patterns. In the case of $KNi^{II}[hcf]_{0.6}[hcc]_{0.4}$ the loss of mass is much higher than in the case of $KCu^{II}[hcf]_{0.6}[hcc]_{0.4}$. Formally, a water content of 12 mol per formula unit $KNi^{II}[hcf]_{0.6}[hcc]_{0.4}$ is obtained. The larger half-widths of the X-ray reflections indicate that the effects of particle size, that is, smaller crystals, may cause a stronger adsorption of water.

Electrochemical Properties. (1) $KCu^{II}[hcf]_{1-x}[hcc]_x$. Figure 5a depicts a cyclic voltammogram of pure $KCu^{II}[hcc]$. Interestingly, an oxidation/reduction system is obtained at a formal potential of ca. 70 mV vs Ag/AgCl. Here, the mid-peak potential of the cyclic voltammograms is taken as the formal potential of the voltammetric system.[51] This system

(51) Scholz, F. Thermodynamics of Electrochemical Reactions. In *Electroanalytical Methods*; Scholz, F., Ed.; Springer: Berlin, 2002.

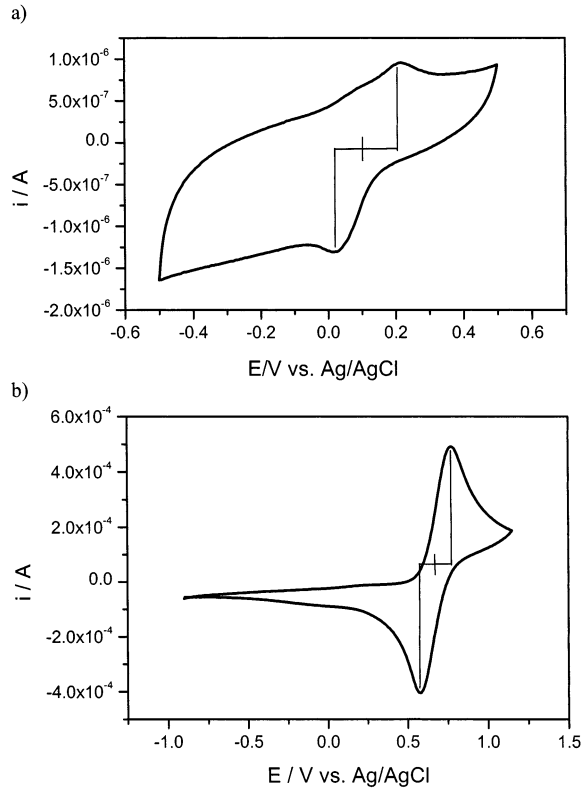

Figure 5. (a) Cyclic voltammogram of $KCu^{II}[hcc]$ in 0.1 M KNO_3 and scan rate 50 mV/s. (b) Cyclic voltammogram of $KCu^{II}[hcf]$ in 0.1 M KNO_3, and scan rate 50 mV/s.

can be assigned to the copper(II)/copper(I) oxidation/reduction. Figure 5b gives a cyclic voltammogram of pure $KCu^{II}[hcf]$. The peak system here is assigned to the oxidation/reduction of the iron ions, as reported by others for copper hexacyanoferrate film electrodes.[1,2] The copper(II) ions are bound much more weakly and retain their individuality much more in the hexacyanocobaltate than in the hexacyanoferrate. The dark brown color of $KCu^{II}[hcf]$ is indicative of a strong charge transfer between copper and iron ions. $KCu^{II}[hcc]$ is a light blue-green color as is typical for copper(II) in an octahedral field of weak ligands. When $KCu^{II}[hcc]$ is suspended in a KCl solution and ascorbic acid is added while the suspension is heated, the blue-green particles are transformed into light yellow particles, as is typical for hexacyanocobaltate(III) salts where the cations are colorless. When the solid is filtered off, it can be reoxidized by heating with diluted nitric acid. The color of the solid is then again light blue-green. The diffuse reflectance spectra transformed into Kubelka−Munk functions of both compounds are given in Figure 6a,b. The strong adsorption band at 700 nm is typical for copper(II) ions, while the weak adsorption below 500 nm is typical for the hexacyanocobaltate(III) ions. Because the reduction and oxidation cycles can be repeated, the chemistry it is based on must be reversible. Because copper(I) ions have no absorption band in the visible range, the following reaction is proposed to occur:

$$KCu^{(II)}[Co^{(III)}(CN)_6] + K^+ + e^- \rightleftarrows K_2Cu^{(I)}[Co^{(III)}(CN)_6] \quad \text{(I)}$$

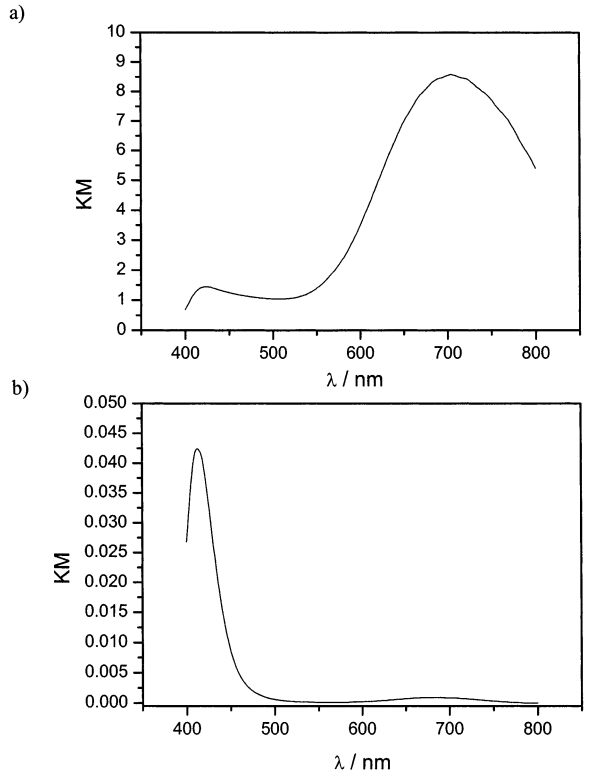

Figure 6. (a) Diffuse reflectance spectrum transformed into Kubelka−Munk function of $KCu^{II}[hcc]$. Compound diluted with $BaSO_4$ at the ratio 1:1. Sample measured versus $BaSO_4$. (b) Diffuse reflectance spectrum transformed into Kubelka−Munk function of $KCu^{I}[hcc]$. Compound undiluted and measured versus $BaSO_4$.

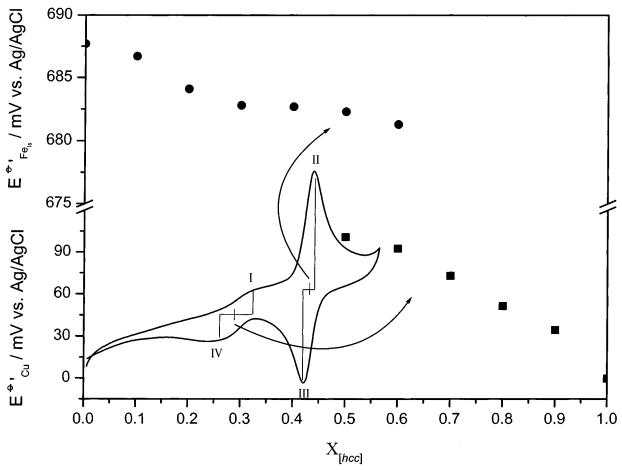

Figure 7. Dependence of the formal potentials of the Cu(I)/Cu(II) system and of the *hcf*(III/II) system of $KCu^{II}[hcf]_{1-x}[hcc]$ on the molar ratio of cobalt. The inset shows a cyclic voltammogram of $KCu^{II}[hcf]_{0.3}[hcc]_{0.7}$, in 0.1 M KNO_3, with a scan rate of 50 mV/s.

Solid solutions of $KCu^{II}[hcf]_{1-x}[hcc]_x$ exhibit two peak systems in CV (cf. inset in Figure 7), one at more negative potentials for copper(II)/copper(I) (marked as I/IV in Figure 7) and one at more positive potentials for *hcf*(III/II) (marked as II/III in Figure 7). The peak system I/IV is present in the range $0.5 \leq x \leq 1$ of hexacyanocobaltate(III), where it shifts by 90 mV. At smaller contents the peaks become very small and the peak potential cannot be measured with sufficient accuracy. The peak system II/III is visible in the range ≤ 0 $x \leq 0.6$. The overall shift here is very small with around 7 mV; however, the shift is very systematic without much scattering (see Figure 7). In both cases the formal potentials decrease with increasing hexacyanocobaltate(III) content. To understand how the substitution of hexacyanoferrate ions by hexacyanocobaltate ions acts on the electrochemistry, it is very interesting to study the dependence of the peak currents of the *hcf*(III/II) system on cobalt contents of the solid solutions. To do so, the powder samples of the solid solutions were carefully mixed in a 1:1 ratio with $KNi^{II}[hcf]$ as an inner standard. The system *hcf*(III/II) in the Ni compound is sufficiently removed from the same system in the Cu compounds so that the ratio of the two systems can be easily determined. The use of the inner standard is necessary because in the voltammetry of immobilized microparticles an exact control of the absolute amount of immobilized substance is not possible. Figure 8 shows that the peak currents of the *hcf*(III/II) system in the Cu-containing solid solutions decrease much more than can be explained by the stoichiometric decrease of the iron content.

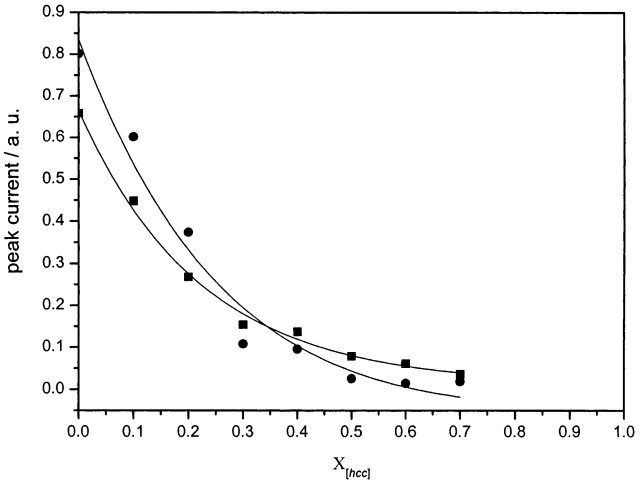

Figure 8. Dependence of the relative peak heights of the oxidation peak (■) and reduction peak (●) of the *hcf*(III/II) system of $KCu^{II}[hcf]_{1-x}[hcc]_x$ on the molar ratio of cobalt. The lines result from an exponential fitting.

(2) $KNi^{II}[hcf]_{1-x}[hcc]_x$. Pure $KNi^{II}[hcf]$ is a greenish-brown color, whereas the pure $KNi^{II}[hcc]$ is a greenish-blue color. The colors of the solid solutions are also greenish-brown. $KNi^{II}[hcc]$ exhibits no electroactive ions in the measurable potential range at the graphite electrode. In cyclic voltammograms of $KNi^{II}[hcf]$ and $KNi^{II}[hcf]_{1-x}[hcc]_x$, the iron ions are electrochemically active and the oxidation/reduction peak system is assigned to *hcf*(III/II) (cf. inset in Figure 9a). The formal potential shifts with the composition as is shown in Figure 9a, with an overall shift of 45 mV. Up to $x = 0.1$ hexacyanocobaltate(III), the formal potential decreases with increasing hexacyanocobaltate(III) content. Then, the formal potential shifts in the positive direction with increasing hexacyanocobaltate(III) content. To study the dependence of peak currents on cobalt content, in the case of the Ni compounds it was necessary to use $KCu^{II}[hcf]$ as the inner standard. The relative peak heights of the oxidation and reduction peaks decrease linearly with increasing hexacyanocobaltate(III) content (Figure 9b). The freshly synthesized $KNi^{II}[hcf]$ compound shows a single peak system. After 2

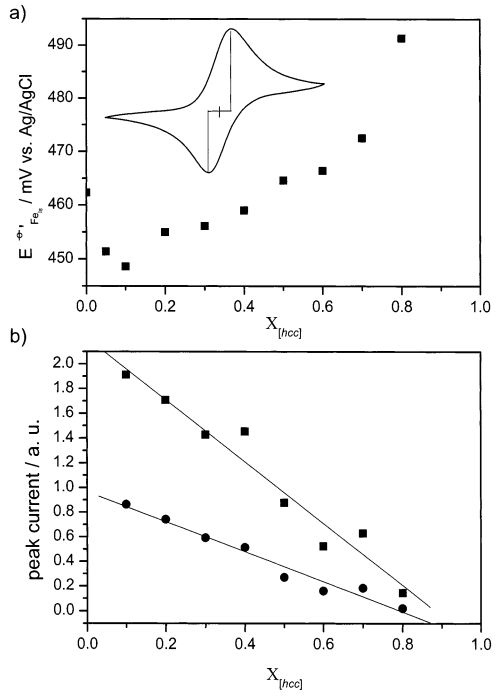

Figure 9. (a) Dependence of the formal potential of the *hcf*(III/II) system of $KNi^{II}[hcf]_{1-x}[hcc]_x$ on the molar ratio of cobalt. The inset shows a cyclic voltammogram of $KNi^{II}[hcf]_{0.3}[hcc]_{0.7}$, in 0.1 M KNO_3, with a scan rate of 50 mV/s. (b) Dependence of the relative peak heights of the oxidation peak (■) and reduction peak (●) of the *hcf*(III/II) system of $KNi^{II}[hcf]_{1-x}[hcc]_x$ on the molar ratio of cobalt. The lines result from a linear fitting.

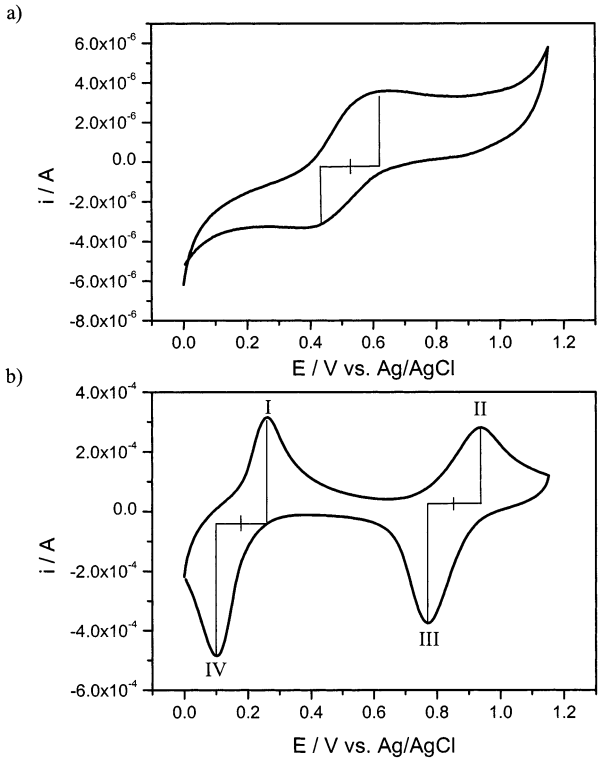

Figure 10. (a) Cyclic voltammogram of fresh synthesized $Fe^{III}[hcc]$ in 0.1 M KNO_3, scan rate 50 mV/s. (b) Cyclic voltammogram of $Fe^{III}[hcc]$ (Prussian green) in 0.1 M KNO_3, scan rate 50 mV/s.

months a second peak system very close to the original system occurs. Such cyclic voltammograms with two peak systems were also described by Kulesza and co-workers for nickel(II) hexacyanoferrate film electrodes.[52,53] When two peak systems occur, the peak heights cannot be measured with sufficient accuracy.

(3) $Fe^{III}[hcf]_{1-x}[hcc]_x$. Pure $Fe^{III}[hcc]$ is a lemon yellow color, whereas the $Fe^{III}[hcf]$ is dark green (known as Prussian green). The solid solutions start with light yellow-green at lower hexacyanoferrate(III) content and become darker with increasing hexacyanoferrate(III) content. To study the dependence of peak currents on cobalt content, in the case of the Fe compounds it was necessary to use $KCu^{II}[hcf]$ as the inner standard. Interestingly, the high-spin iron is electrochemically active also in $Fe^{III}[hcc]$, but the peak heights of the oxidation and reduction of these high-spin iron ions are 2 orders of magnitude smaller than those in Prussian green $Fe^{III}[hcf]$, whereas the concentration of the high-spin iron ions is the same in both compounds (cf. peak system marked as I/IV in Figure 10a,b). It must be mentioned at this point that the cyclic voltammogram depicted in Figure 10a is obtainable only with freshly synthesized $Fe^{III}[hcc]$. After 2 days, the peak system of low-spin iron appears, obviously because of a partial decomposition to Prussian green (visible in the color change to light green). The formal potential of the high-spin iron system (marked as I/IV in Figure 10a,b) shifts in the positive direction with increasing hexacyanocobaltate(III) content. The overall shift is about 130 mV and hence higher than those in all other systems that are described here (Figure 11a). In contrast to that, the formal potential of the low-spin iron system (marked as II/III in Figure 10b) shifts only slightly with a minimum at a hexacyanocobaltate(III) content of $x = 0.2$ (cf. Figure 11b). This peak system vanishes at a hexacyanocobaltate(III) content above $x = 0.6$. The relative peak heights for both peak systems decrease with increasing hexacyanocobaltate(III) content (see Figure 12a,b).

Magnetic Properties. All solid solutions were investigated using zero field-cooled magnetization in a temperature range of 5−35 K. In the case of the $KCu^{II}[hcf]_{1-x}[hcc]_x$ series, when $x = 0$ ($KCu^{II}[hcf]$), the interaction between the unpaired electrons on the e_g orbitals of Cu^{II} and the unpaired electrons on t_{2g} orbitals of Fe^{III} leads to a ferromagnetic ordering with a T_c of 16 K. Co^{III} exhibits no unpaired electrons; that is, there is no interaction with unpaired electrons of Cu^{II} possible. When $x = 0.8$ ($KCu^{II}[hcf]_{0.2}[hcc]_{0.8}$), the T_c was found to be 14 K. For the intermediate values of x, the solid solutions showed a T_c of ∼14−16 K (cf. Table 3), which is the range of the transition temperature of the constituent copper hexacyanoferrate. A plot of M vs H is shown in Figure 13, typical for the $KCu^{II}[hcf]_{1-x}[hcc]_x$ series. The width of the hysteresis loop is small, indicating that the bulk magnetization is not so strong. The H_c and H_{REM} values are quite small. The $M(H)$ plots do not saturate for any of these samples, implying that the field H_{app} is not enough to turn the domains completely along its direction.

(52) Bacskai, J.; Martinusz, K.; Czirok, E.; Inzelt, G.; Kulesza, P. J.; Malik, A. *J. Electroanal. Chem.* **1995**, *385*, 241−248.
(53) Malik, M. A.; Miecznikowski, K.; Kulesza, P. J. *Electrochim. Acta* **2000**, *45*, 3777−3784.

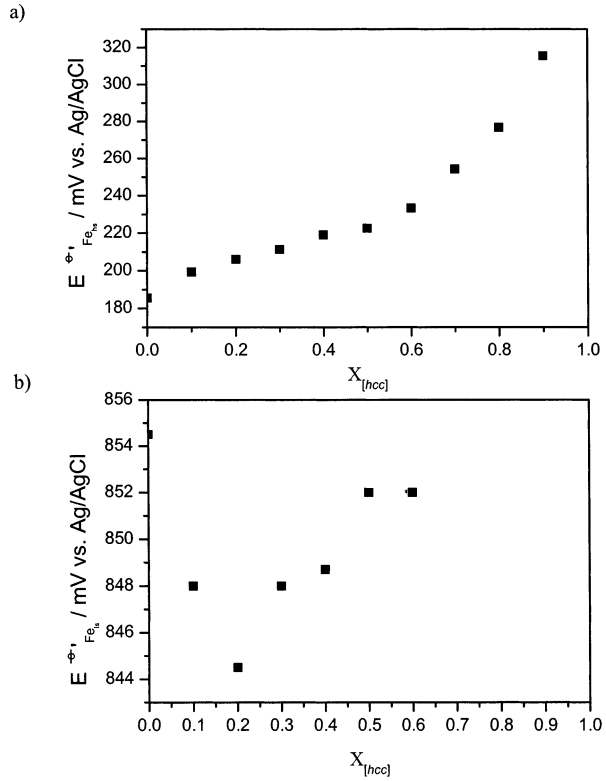

Figure 11. (a) Dependence of the formal potential of the high-spin Fe(II)/Fe(III) system of $Fe^{III}[hcf]_{1-x}[hcc]_x$ on the molar ratio of cobalt. (b) Dependence of the formal potential of the *hcf*(III/II) (low-spin) system of $Fe^{III}[hcf]_{1-x}[hcc]_x$ on the molar ratio of cobalt.

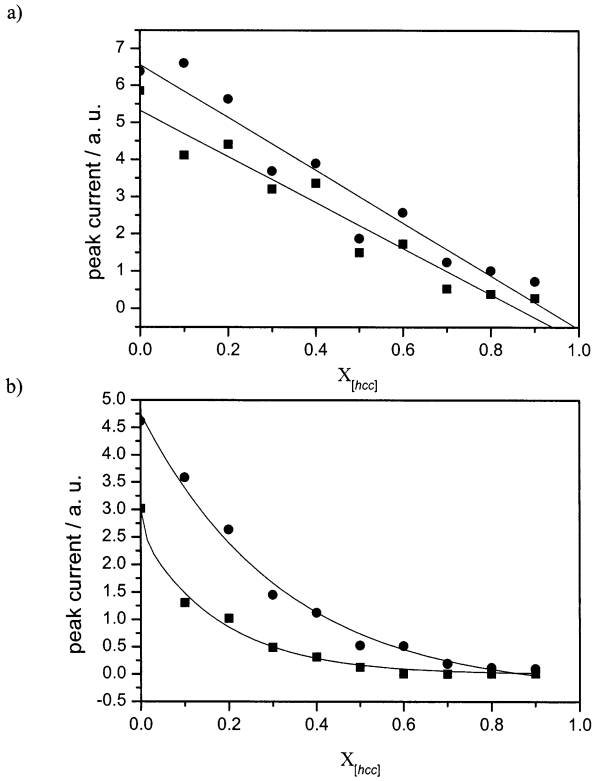

Figure 12. (a) Dependence of the relative peak heights of the oxidation peak (■) and reduction peak (●) of the high-spin Fe(II)/Fe(III) system of $Fe^{III}[hcf]_{1-x}[hcc]_x$ on the molar ratio of cobalt. The lines result from a linear fitting. (b) Dependence of the relative peak heights of the oxidation peak (■) and reduction peak (●) of the *hcf*(III/II) (low-spin) system of $Fe^{III}[hcf]_{1-x}[hcc]_x$ on the molar ratio of cobalt. The lines result from an exponential fitting.

On the other hand, in the case of the series $KNi^{II}[hcf]_{1-x}[hcc]_x$, the T_c was found to increase with decreasing x, showing a maximum of 23 K for $x = 0.0$ ($KNi^{II}[hcf]$) (cf. Table 4 and Figure 14). In the case of Ni^{II} two unpaired electrons on e_g orbitals can interact with unpaired electrons on t_{2g} orbital of Fe^{III}. This could be an explanation for the higher dependency of T_c on the amount of Fe^{III}.

For the series $Fe^{III}[hcf]_{1-x}[hcc]_x$, the highest T_c of 22.5 K was observed for $x = 0.0$ (i.e., without Co^{III}). Such high T_c was observed because of the potential exchange interactions between the unpaired electrons on e_g orbitals of Fe^{III} and t_{2g} electrons of low-spin Fe^{III}. $KFe^{III}[hcc]$ (i.e., when $x = 1$) was found to undergo a magnetic transition at 11 K because of the absence of paramagnetic spin on central Co^{III}. Thus, the intermediate solid solutions showed a monotonic decrease in T_c from 22.5 to 11 K (cf. Table 5 and Figure 15) as the cobalt content x is increased from $x = 0$ to $x = 1$, which appears logical. In contrast to the $KCu^{II}[hcf]_{1-x}[hcc]_x$ series, here, the H_c values are appreciable, ranging from ~40 Oe for $x = 0.9$ and $x = 0.8$ to as high as 770 Oe for $x = 0$ at 4.5 K. As a representative $M(H)$ plot for $x = 0$ ($Fe^{III}[hcf]$) is shown in Figure 16.

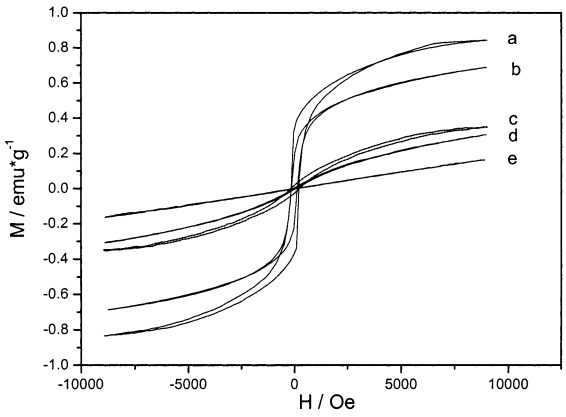

Figure 13. Hysteresis loops for $KCu^{II}[hcf]_{1-x}[hcc]_x$ at 4.5 K. (a) $KCu^{II}[hcf]$, (b) $KCu^{II}[hcf]_{0.8}[hcc]_{0.2}$, (c) $KCu^{II}[hcf]_{0.5}[hcc]_{0.5}$, (d) $KCu^{II}[hcf]_{0.3}[hcc]_{0.7}$, and (e) $KCu^{II}[hcf]_{0.1}[hcc]_{0.9}$.

Table 3. T_c Values of Solid Solutions of $KCu^{II}[hcf]_{1-x}[hcc]_x$

compound	transition temp (K)	compound	transition temp (K)
$KCu[Co(CN)_6]$		$KCu[Co_{0.6}Fe_{0.4}(CN)_6]$	15
$KCu[Co_{0.9}Fe_{0.1}(CN)_6]$		$KCu[Co_{0.5}Fe_{0.5}(CN)_6]$	15
$KCu[Co_{0.8}Fe_{0.2}(CN)_6]$	14	$KCu[Co_{0.2}Fe_{0.8}(CN)_6]$	15
$KCu[Co_{0.7}Fe_{0.3}(CN)_6]$	15	$KCu[Fe(CN)_6]$	16

Conclusions

Substituting electroactive hexacyanoferrate(III) ions in solid metal hexacyanoferrates(III) by electroinactive hexacyanocobaltate(III) ions affects the formal potentials of both the *hcf*(III/II) system and the formal potential of the nitrogen-coordinated metal ions, provided that they are electroactive. From the experiments follows that the substitution of iron by cobalt affects only slightly the formal potential of the *hcf*(III/II) system because the nearest iron ion will be six bonds away from a cobalt ion. The same substitution has a

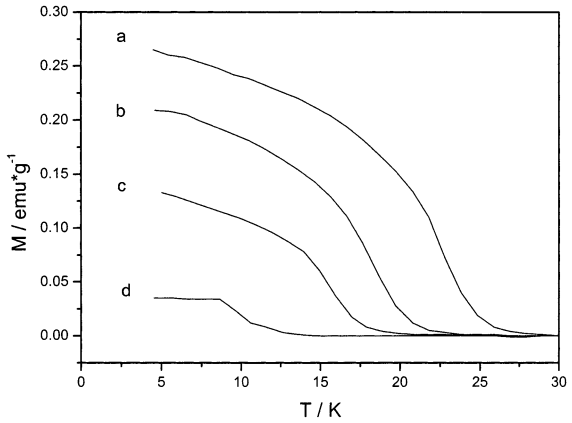

Figure 14. Field-cooled magnetization plots for $KNi^{II}[hcf]_{1-x}[hcc]_x$ at 500 Oe. (a) $KNi^{II}[hcf]$, (b) $KNi^{II}[hcf]_{0.8}[hcc]_{0.2}$, (c) $KNi^{II}[hcf]_{0.7}[hcc]_{0.3}$, and (d) $KNi^{II}[hcf]_{0.5}[hcc]_{0.5}$.

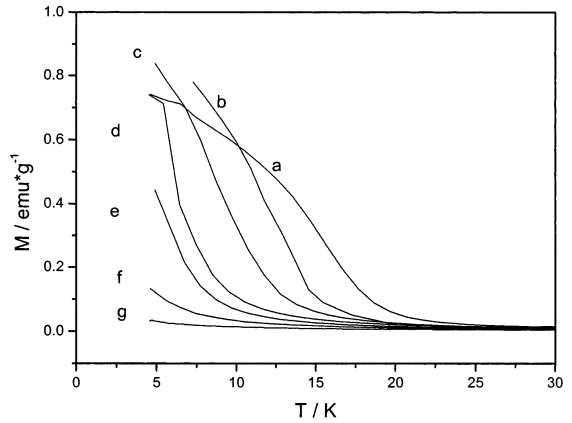

Figure 15. Field-cooled magnetization plots for $Fe^{III}[hcf]_{1-x}[hcc]_x$ at 500 Oe. (a) $Fe^{III}[hcf]$, (b) $Fe^{III}[hcf]_{0.9}[hcc]_{0.1}$, (c) $Fe^{III}[hcf]_{0.7}[hcc]_{0.3}$, (d) $Fe^{III}[hcf]_{0.5}[hcc]_{0.5}$, (e) $Fe^{III}[hcf]_{0.4}[hcc]_{0.6}$, (f) $Fe^{III}[hcf]_{0.2}[hcc]_{0.8}$, and (g) $Fe^{III}[hcc]$.

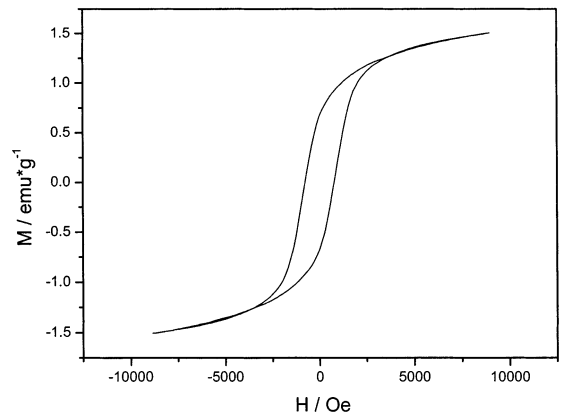

Figure 16. Hysteresis loop for $Fe^{II}[hcf]$ at 4.5 K.

larger effect on the system of the nitrogen-coordinated metal ions, that is, copper(II) or high-spin iron(III) ions, because they are only separated by three bonds from the cobalt ions. The results obtained for the solid solutions of hexacyanoferrate−hexacyanocobaltates have interesting implications for a deeper understanding of the isomerization of iron hexacyanochromate to chromium hexacyanoferrate, an electrochemically driven reaction described earlier.[54] This reaction does not result in any shift of the formal potentials of the hexacyanoferrate and hexacacyanochromate systems, which must be expected when solid solutions are intermediates. Because this was not observed, the reaction must proceed in a thin layer of a progressing reaction front, completely in line with model calculations of similar systems.[55]

Table 4. T_c Values of Solid Solutions of $KNi^{II}[hcf]_{1-x}[hcc]_x$

compound	transition temp (K)	compound	transition temp (K)
$KNi[Co(CN)_6]$		$KNi[Co_{0.2}Fe_{0.8}(CN)_6]$	19
$KNi[Co_{0.9}Fe_{0.1}(CN)_6]$		$KNi[Co_{0.1}Fe_{0.9}(CN)_6]$	21
$KNi[Co_{0.5}Fe_{0.5}(CN)_6]$	13	$KNi[Fe(CN)_6]$	23
$KNi[Co_{0.3}Fe_{0.7}(CN)_6]$	16		

Table 5. T_c Values of Solid Solutions of $\{Fe^{III}[hcf]_{1-x}[hcc]_x\}$

compound	transition temp (K)	compound	transition temp (K)
$Fe[Co(CN)_6]$	11	$Fe[Co_{0.4}Fe_{0.6}(CN)_6]$	17
$Fe[Co_{0.9}Fe_{0.1}(CN)_6]$	12	$Fe[Co_{0.3}Fe_{0.7}(CN)_6]$	18
$Fe[Co_{0.8}Fe_{0.2}(CN)_6]$	12	$Fe[Co_{0.2}Fe_{0.8}(CN)_6]$	19
$Fe[Co_{0.7}Fe_{0.3}(CN)_6]$	12.5	$Fe[Co_{0.1}Fe_{0.9}(CN)_6]$	20
$Fe[Co_{0.6}Fe_{0.4}(CN)_6]$	13.5	$Fe[Fe(CN)_6]$	22.5
$Fe[Co_{0.5}Fe_{0.5}(CN)_6]$	14.5		

In the three series of solid solutions studied, there is no uniform shift of formal potentials of the redox systems with increasing hexacyanocobaltate content. There is also no uniform behavior of the peak currents as a function of the hexacyanocobaltate(III) content. The linear decrease of the peak current of the high-spin iron system with increasing cobalt content in $Fe^{III}[hcf]_{1-x}[hcc]_x$, as well as the exponential decrease of the peak currents of low-spin iron in $KCu^{II}[hcf]_{1-x}[hcc]_x$ and $Fe^{III}[hcf]_{1-x}[hcc]_x$, must be the result of a decreasing rate of charge propagation. Only in the case of the $KNi^{II}[hcf]_{1-x}[hcc]_x$ series do the peak currents of the low-spin iron decrease proportional to their concentration. Further studies are necessary to understand the effect of substitution on electron and possibly also on cation propagation.

The very interesting deviation of the lattice constants from linearity (Figure 3) goes along with the shifts of the formal potentials of the electrochemical systems upon varying the composition. A possible explanation is that the substitution of iron by cobalt indeed affects the bonding in the entire network. Thus, the formation of these mixed crystals involves genuine chemical changes. These deviations from ideality have not yet been shown for the hexacyanometalate systems. Certainly, it is important to know all these effects because only this allows synthesis of tailored compounds.

The X-ray Rietveld refinements of all the studied solid solutions and pure compounds confirmed the Keggin model for Prussian blue. Hence, the structure is much more simple compared to that proposed by Ludi for Prussian blue. The most significant result from the structure refinement is the obvious disorder of the potassium sites. Whereas in the case of the copper-containing compounds the potassium ions are situated in the centers of the cubes, in the case of nickel containing compounds they are eccentrically located. The present study also shows that water molecules are not a lattice

(54) Dostal, A.; Schröder, U.; Scholz, F. *Inorg. Chem.* **1995**, *34*, 1711−1717.
(55) Hermes, M.; Lovric, M.; Hartl, M.; Retter, U. *J. Electroanal. Chem.* **2001**, *501*, 193−204.

constituent of the metal hexacyanometalates. This fact has the very important implication that the alkali metal ions must exist unhydrated in the solid compounds. Therefore, the entropy change occurring when the alkali metal ions enter the solid compounds in insertion electrochemical reactions is determined by their complete dehydration.[56] Further, because there is even no partial hydration cloud around the metal ions in the solid compounds, the mobility of alkali metal ions in the channels of the solid metal hexacyanometalates should increase with decreasing alkali metal ion radius, thus providing the highest mobility in the case of lithium ions. In a separate paper on the impedance spectroscopy of these compounds we will show that this is indeed the case.

Acknowledgment. We acknowledge the support by Deutsche Forschungsgemeinschaft and Fonds der Chemischen Industrie.

Supporting Information Available: Crystallographic data in CIF format. This material is available free of charge via the Internet at http://pubs.acs.org.

IC0201654

(56) Bàrcena Soto, M.; Scholz, F. *J. Electroanal. Chem*., in press.